Design of H-inf Controller with Tuning of Weights Using Particle Swarm Optimization Method

H. I. A.li, Member IAENG, S. B. Mohd Noor, M. H. Marhaban, S. M. Bashi

Abstract-- **In this paper a new method based on a particle swarm optimization (PSO) algorithm for tuning the weighing functions parameters to design an H_∞ controller is presented. The PSO algorithm is used to minimize the infinity norm of the transfer function of the nominal closed loop system to obtain the optimal parameters of the weighting functions. This method is applied to a typical industrial pneumatic servo actuator with system uncertainty and wide range of load variation to illustrate the design procedure of the proposed method. It is shown that the proposed method can simplify the design procedure of H_∞ control to obtain optimal robust controller for pneumatic servo actuator system.**

Index Terms—**Robust control, PSO, H_∞ control, Pneumatic actuator, parametric uncertainty.**

I. INTRODUCTION

H_∞ is one of the best known techniques available nowadays for robust control. It is a method in control theory for optimal controller design. Basically, it is an optimization method that takes into consideration a strong definition of the mathematical way to express the ability to include both classical and robust control concepts within a single design framework. It is known that H_∞ control is an effective method for attenuating disturbances and noise that appear in the system. It is one of the best techniques in linear control system. The "*H*" stands for Hardy space. "*Infinity*" means that it is designed to accomplish minimax restrictions in the frequency domain. The H_∞ norm of a dynamic system is the maximum amplification that the system can make to the energy of the input signal [1, 2].

Manuscript received January 26, 2010.

H. I. Ali. is with the Electrical and Electronic Engineering Department, University Putra Malaysia, Serdand, Selangor, Malaysia, (corresponding author to provide phone: 0060-17-2579348; fax: 603-8946-6327; e-mail: hazemcontrol2001@ yahoo.com).

S. B. Mohd Noor, is with the Electrical and Electronic Engineering Department, University Putra Malaysia, Serdand, Selangor, Malaysia, (e-mail: samsul@ eng.upm.edu.my).

S. M. Bashi, is with the Electrical and Electronic Engineering Department, University Putra Malaysia, Serdand, Selangor, Malaysia, (e-mail: senan@ eng.upm.edu.my).

M. H. Marhaban, is with the Electrical and Electronic Engineering Department, University Putra Malaysia, Serdand, Selangor, Malaysia, (e-mail: hamiruce@ eng.upm.edu.my).

One of the most important parts and a key step in the design of the H_∞ controller is the selection of weighting functions and weighting gains for specific design problems. This is not an easy procedure and often needs many iterations as well as fine-tuning. Furthermore, it is hard to find a general formula for the weighting functions that will work in every case. Therefore, to obtain a good control design it is necessary to use suitable selected and tuned weighting functions [3].

In this paper, a method for the position control design of a pneumatic servo actuator system-using H_∞ controller is presented. The PSO algorithm is used to find the optimal values of the parameters of the weighting functions that lead to obtain the optimal H_∞ controller by minimizing the infinity norm of the transfer function matrix of the nominal closed loop system. The PSO method is used because of its simplicity and ease of implementation. The structured (parametric) uncertainty is considered in the design.

II. Particle Swarm Optimization Algorithm (PSO)

PSO is one of a powerful optimization method with high efficiency in comparison to other methods. It is a stochastic Evolutionary Computation technique based on the movement and intelligence of swarms. The PSO mechanism is initialized with a population of random solutions and searches for optima by updating generations. A swarm consists of N particles that are moving around in a D dimensional search space. Each particle keeps track of its coordinates in the space of the problem, which are associated with the best solution (best fitness) it has achieved so far. The best particle in the population is denoted by (global best), while the best position that has been visited by the current particle is denoted by (local best). The global best individual connects all members of the population to one another. That is, each particle is influenced by every best performance of any member in the entire population. The local best individual is seen as the ability for particles to remember past personal success. The particle swarm optimization concept involves, at each time step, changing the velocity of each particle towards its global best and local best locations. The particles are manipulated according to the following equations of motion [4,5, 6, 7]:

$$v_i^{k+1} = h \times v_i^k + c_1 \times rand \times (x_i^b - x_i^k) + c_2 \times rand \times (x_i^g - x_i^k) \qquad (1)$$

(Advance online publication: 25 May 2011)

$$x_i^{k+1} = x_i^k + v_i^{k+1} \quad (2)$$

where v_i^k is the particle velocity, x_i^k is the current particle position, w is the inertia weight, x_i^b and x_i^g are the best value and the global best value, *rand* is a random function between 0 and 1, c_1 and c_2 are learning factors.

The PSO requires only a few lines of computer code to realize PSO algorithm. Also it is a simple concept, easy to implement, and computationally efficient algorithm [8, 9].

III. PNEUMATIC SERVO ACTUATOR MODEL

Consider the pneumatic servo actuator system given in [10, 11]. This system is widely used in industrial applications because it is cheap, clean, lightweight, easy to maintain and it provides a high degree of compliance. On the other hand, it is difficult to achieve precise position for such systems because of the friction forces and the nonlinearity due to the compressibility of the air. Further, the variation in thermodynamic conditions causes an uncertainty in a number of model's parameters. Therefore, it is a need to apply the robust control techniques to control such as systems. Fig. 1 shows the schematic diagram of the pneumatic servo actuator. The source of power used in this type of actuator is compressed air supplied to the jet pipe, and distributed between the two ways pneumatic cylinder as the jet pipe turns [12, 13]. The valve and actuator characteristics can be linearized about the operating point (nominal point) to yield the following fourth order linear model of the open loop system:

$$y_P(s) = G_p(s)U(s) - G_d(s)F_d(s) \quad (3)$$

where

$$G_p(s) = \frac{2K\dfrac{\gamma R T_s A_p}{MV_o}}{s(\tau_v s+1)\left(s^2 + (\dfrac{f}{M} - \dfrac{\gamma R T_s L_a}{MV_o})s + (\dfrac{2\gamma(A_p)^2 P_i}{MV_o} - \dfrac{\gamma R T_s L_a A_p f}{MV_o})\right)} \quad (4)$$

and

$$G_d(s) = \frac{\dfrac{1}{M}}{s(\tau_v s+1)\left(s^2 + (\dfrac{f}{M} - \dfrac{\gamma R T_s L_a}{MV_o})s + (\dfrac{2\gamma(A_p)^2 P_i}{MV_o} - \dfrac{\gamma R T_s L_a A_p f}{MV_o})\right)} \quad (5)$$

where y_p is the piston displacement, u is the valve input voltage, F_d is the disturbing load, K is the valve constant, A_p is the piston area, V_o is the air volume, τ_v is the valve time constant, R is the gas constant, γ is the specific heat ratio, T_s is the temperature, f is the viscous friction coefficient. The nominal values of system parameters and their variation range are given in Table 1.

The coefficient L_a is typically very small compared to other terms of the system and has a very small effect on the system performance. In particular, when under chocked flow conditions, L_a=0. The maximum mass flow rate occurs under chocked flow conditions and the unchecked flow rate is bounded by the chocked flow rate. Also, since the dynamics of the control valve are much faster than the required response of the servo actuator, the relationship between control signal and valve can be approximated by a proportional gain as mentioned in [14, 15]. Fig. 2 shows the block diagram of the pneumatic servo actuator system.

The frequency characteristic of the pneumatic actuator with all parameters uncertainty is shown in Fig. 3. These characteristics show that the system bandwidth decreases when the load increases, until the system becomes slower. Also the phase margin decreases when the load increases and this makes the system to oscillate and be unstable system.

IV. H$_\infty$ CONTROLLER DESIGN WITH PARAMETRIC UNCERTAINTY

The pneumatic servo actuator system can be represented as shown in Fig. 4. The parameters *a*, *b* and *c* can be assumed to be:

$$a = \frac{MV_o}{2K_p K A_p \alpha RT}, \; b = \frac{fV_o}{2K_p K A_p \alpha RT}, \text{ and } c = \frac{AP_o}{K_p KRT} \quad (6)$$

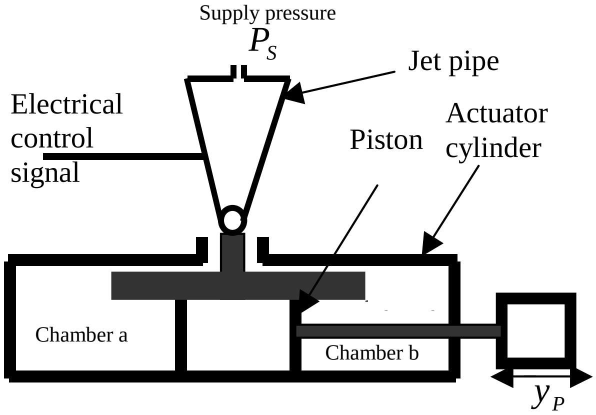

Fig. 1. Schematic diagram of pneumatic servo actuator system.

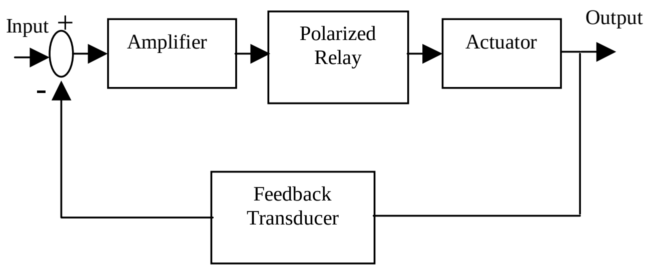

Fig. 2. Block diagram of pneumatic servo actuator system

Table I. The nominal system model parameters and their range

Uncertain Parameter	A_p m^2	$\frac{R}{J}$ $kg.K^\circ$	$V_o(m^3)$ $\times 10^4$	P_i bar	M kg	f $\frac{N.\sec}{m}$	K $\frac{kg}{s.V}\times 10^3$	Ts K°	γ	K_P V/m
Minimum value			1.5		0.1	50	3.2			
Nominal value	0.005	287	2.5	3	1	60	3.4	293.15	1.4	400
Maximum value			4	4	5, 100	80				

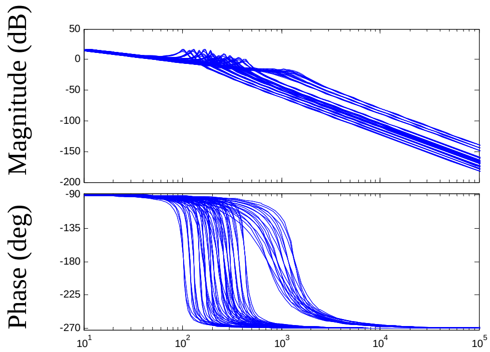

Fig. 3. Frequency response characteristics of the system with parameters uncertainty and wide range of load variation.

The three physical parameters *a*, *b* and *c* are unknown exactly, therefore, they can be assumed to be within the range of the system parameters in Table I, That is:

$$a = \bar{a}(1+\delta_a p_a)\,,\ b = \bar{b}(1+\delta_b p_b)\ \text{ and }\ c = \bar{c}(1+\delta_c p_c) \tag{7}$$

where $\bar{a} = 0.0664\times 10^{-5}$ and 0.1327×10^{-4} for small and wide ranges of load variation, respectively, $\bar{b} = 0.1295\times 10^{-4}$ and $\bar{c} = 0.01585$ are the nominal values of *a*, *b* and *c*. p_a, p_b and p_c and δ_a, δ_b and δ_c represent the possible perturbations on these parameters. In this work we let $p_a = 0.99999991$ and 0.999246 for the two ranges of load variation, respectively, $p_b = 0.64$, $p_c = 0.174$ and $-1 \le \delta_a, \delta_b, \delta_c \le 1$. Note that this represents up to 99.999991% and 99.9246% uncertainty in the parameter *a*, 64% uncertainty in the parameter *b* and 17.4% uncertainty in the parameter *c*.

The three constant blocks in Fig. 4 have been replaced by block diagrams in terms of $\bar{a}, p_a, \delta_a$, etc., in a unified approach. The quantity $(\frac{1}{a})$ can be represented as an upper linear fractional transformation (LFT) in δ_a as:

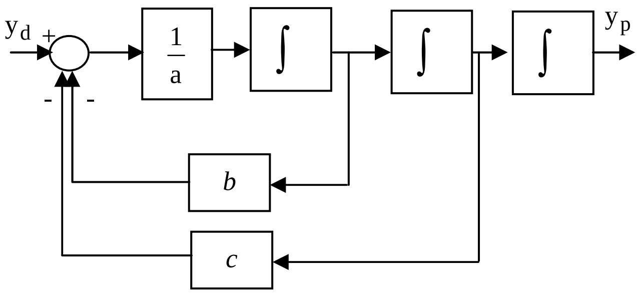

Fig. 4. Block diagram of pneumatic servo actuator system with its main parameters

$$\frac{1}{a} = \frac{1}{\bar{a}(1+p_a\delta_a)} = \frac{1}{\bar{a}} - \frac{p_a}{\bar{a}}\delta_a(1+p_a\delta_a)^{-1} = F_u(M_a,\delta_a) \tag{8}$$

with

$$M_a = \begin{bmatrix} -p_a & \frac{1}{\bar{a}} \\ -p_a & \frac{1}{\bar{a}} \end{bmatrix} \tag{9}$$

Similarly, the parameters *b* and *c* can be represented as an upper LFT in δ_b, and δ_c as:

$$b = F_u(M_b,\delta_b) \tag{10}$$

with

$$M_b = \begin{bmatrix} 0 & \bar{b} \\ p_b & \bar{b} \end{bmatrix} \tag{11}$$

and

$$c = F_u(M_c,\delta_c) \tag{12}$$

with

$$M_c = \begin{bmatrix} 0 & \bar{c} \\ p_c & \bar{c} \end{bmatrix} \tag{13}$$

(Advance online publication: 25 May 2011)

Fig. 5 shows the representation of uncertain parameters as LFTs. The relationship between the input signals, w the output signals, z can be expressed as [1]:

$$z = F_u(N,\Delta) = [N_{22} + N_{21}\Delta(1 - N_{11}\Delta)^{-1} N_{12}]w \qquad (14)$$

where N may represent M_a or M_b or M_c and Δ may represent δ_a or δ_b or δ_c. The inputs and outputs of δ_a, δ_b and δ_c are denoted as y_a, y_b, y_c and u_a, u_b, u_c, respectively, as shown in Fig. 6.

The equations relating all inputs to corresponding outputs around the uncertain parameters can be obtained as:

$$\begin{bmatrix} y_a \\ v_a \end{bmatrix} = M_a \begin{bmatrix} u_a \\ u - v_b - v_c \end{bmatrix} \qquad (15)$$

$$\begin{bmatrix} y_b \\ v_b \end{bmatrix} = M_b \begin{bmatrix} u_b \\ \ddot{y}_p \end{bmatrix} \qquad (16)$$

$$\begin{bmatrix} y_c \\ v_c \end{bmatrix} = M_c \begin{bmatrix} u_{ac} \\ \dot{y}_p \end{bmatrix} \qquad (17)$$

where

$$u_a = \delta_a y_a\,,\; u_b = \delta_b y_b\,,\; u_c = \delta_c y_c \qquad (18)$$

The system state space representation can be expressed as:

$$x_1 = y_p\,, x_2 = \dot{y}_p = \dot{x}_1 \text{ such that } \dot{x}_2 = \ddot{y}_p = \ddot{x}_1 \qquad (19)$$

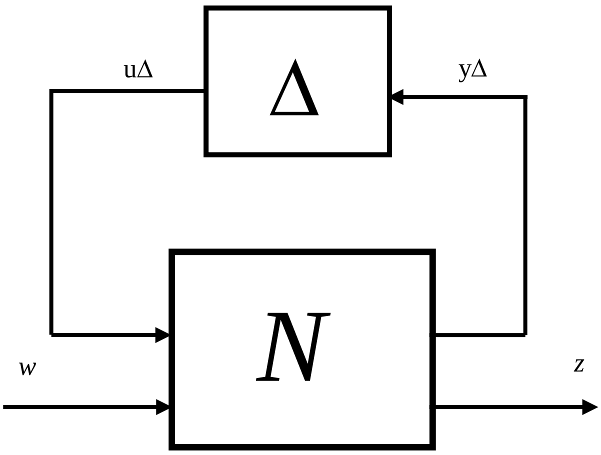

Fig. 5. General LFT representation

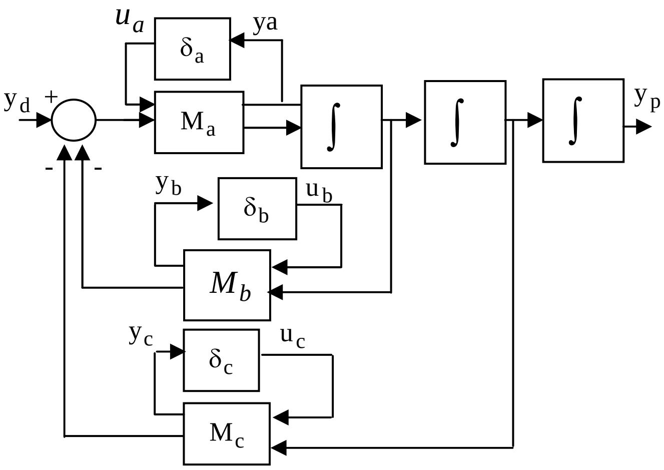

Fig. 6. Block diagram of the pneumatic system with uncertain parameters

As a result, the following equations can be obtained:

$$\dot{x}_1 = x_2 \qquad (20)$$

$$\dot{x}_2 = x_3 \qquad (21)$$

$$\dot{x}_3 = -p_a u_a + \frac{1}{\bar{a}}(u - v_b - v_c) \qquad (22)$$

$$y_a = p_b u_b + \bar{b} x_3 \qquad (23)$$

$$v_c = p_c u_c + \bar{c} x_2 \qquad (24)$$

The equations governing the pneumatic servo actuator system dynamic behaviour can be obtained as:

$$\begin{bmatrix} \dot{x}_1 \\ \dot{x}_2 \\ \dot{x}_3 \\ y_a \\ y_b \\ y_c \\ y_p \end{bmatrix} = \begin{bmatrix} 0 & 1 & 0 & 0 & 0 & 0 & 0 \\ 0 & 0 & 1 & 0 & 0 & 0 & 0 \\ 0 & \frac{-\bar{c}}{\bar{a}} & \frac{-\bar{b}}{\bar{a}} & -p_a & \frac{-p_b}{\bar{a}} & \frac{-p_c}{\bar{a}} & \frac{1}{\bar{a}} \\ 0 & \frac{-\bar{c}}{\bar{a}} & \frac{-\bar{b}}{\bar{a}} & -p_a & \frac{-p_b}{\bar{a}} & \frac{-p_c}{\bar{a}} & \frac{1}{\bar{a}} \\ 0 & 0 & \bar{b} & 0 & 0 & 0 & 0 \\ 0 & \bar{c} & 0 & 0 & 0 & 0 & 0 \\ 1 & 0 & 0 & 0 & 0 & 0 & 0 \end{bmatrix} \begin{bmatrix} x_1 \\ x_2 \\ x_3 \\ u_a \\ u_b \\ u_c \\ u \end{bmatrix} \qquad (25)$$

and

$$\begin{bmatrix} u_a \\ u_b \\ u_c \end{bmatrix} = \begin{bmatrix} \delta_a & 0 & 0 \\ 0 & \delta_b & 0 \\ 0 & 0 & \delta_c \end{bmatrix} \begin{bmatrix} y_a \\ y_b \\ y_c \end{bmatrix} \qquad (26)$$

Let G_p denotes the input/output dynamics of the pneumatic system, which takes into account the uncertainty of parameters. G_p has four inputs (u_a, u_b, u_c, u), four outputs (y_a, y_b, y_c, y_p) and three states (x_1, x_2, x_3).

The state space representation of G_p is [2]:

$$G_p = \begin{bmatrix} A & B_1 & B_2 \\ C_1 & D_{11} & D_{12} \\ C_2 & D_{21} & D_{22} \end{bmatrix} \qquad (27)$$

where

$$A=\begin{bmatrix}0 & 1 & 0\\ 0 & 0 & 1\\ 0 & \frac{-\bar{c}}{\bar{a}} & \frac{-\bar{b}}{\bar{a}}\end{bmatrix},\ B_1=\begin{bmatrix}0 & 0 & 0\\ 0 & 0 & 0\\ -p_a & \frac{-p_a}{\bar{a}} & \frac{-p_c}{\bar{a}}\end{bmatrix},$$

$$B_2=\begin{bmatrix}0\\ 0\\ \frac{1}{\bar{a}}\end{bmatrix},\ C_1=\begin{bmatrix}0 & \frac{-\bar{c}}{\bar{a}} & \frac{-\bar{b}}{\bar{a}}\\ 0 & 0 & \bar{b}\\ 0 & \bar{c} & 0\end{bmatrix},$$

$$D_{11}=\begin{bmatrix}0\\ 0\\ \frac{1}{\bar{a}}\end{bmatrix},\ D_{12}=\begin{bmatrix}\frac{1}{\bar{a}}\\ 0\\ 0\end{bmatrix},\ C_2=\begin{bmatrix}1 & 0 & 0\end{bmatrix},$$

$$D_{21}=\begin{bmatrix}0 & 0 & 0\end{bmatrix},\ D_{22}=0 \qquad (28)$$

It is clear that the system matrix G_p has no uncertain parameters and depends only on $\bar{a},\bar{b},\bar{c},p_a,p_b,p_c$ and on the original system parameters. The uncertain behaviour of the original system can be described by the upper LFT representation as:

$$y_p = F_u(G_p,\Delta)u \qquad (29)$$

with diagonal uncertainty matrix Δ as shown in Fig. 7, where Δ is the unknown matrix, which is called the uncertainty matrix with fixed structure (structured uncertainty).

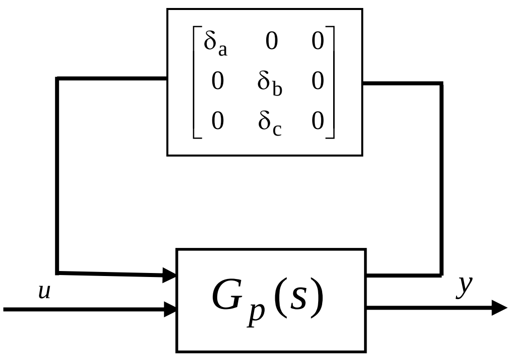

Fig. 7. Upper LFT representation of the system

A. Bilinear Transform and Weighting Functions Selection

Since the proposed system has *jw*-axis pole, the H_∞ controller, if it is reliably computed, would have a marginally stable closed loop pole at the corresponding *jw*-axis location. This problem leads to singularities in the equations that determine the state space realization of H_∞ control law. Therefore, a simple bilinear transform has been found to be extremely useful when used with robust control synthesis. This transformation can be formulated as a *jw*-axis pole shifting transformation [16]:

$$s=\frac{\hat{s}+p_{b1}}{\frac{\hat{s}}{p_{b2}}+1} \qquad (30)$$

where $p_{b1}<0$ and selected to be 0.1, p_{b2} is selected to be infinity. This is equivalent to simply shifting the *jw*-axis by p_{b1} units to the left. The H_∞ controller was obtained for the shifted system then it was shifted back to the right with the same units.

The design requirements and objectives for pneumatic servo actuator system in this work is to find a linear, output feedback control $u(s)=K(s)y_p(s)$, which ensures that the closed loop system will be internally stable. Also, the required closed loop system performance should be achieved for the nominal plant G_p.

To obtain a good control design, it is necessary to select suitable weighting functions. The performance and control weighting functions formulas that have been used in this work are [16]:

$$W_p(s)=\frac{\beta(\alpha s^2+2\zeta_1 w_c\sqrt{\alpha}s+w_c{}^2)}{(\beta s^2+2\zeta_2 w_c\sqrt{\beta}s+w_c{}^2)} \qquad (31)$$

$$W_u(s)=\frac{s^2+2\frac{w_{bc}}{\sqrt{M_u}}s+\frac{w^2{}_{bc}}{M_u}}{\varepsilon s^2+2\sqrt{\varepsilon}w_{bc}s+w^2{}_{bc}} \qquad (32)$$

where β is the d.c. gain of the function which controls the disturbance rejection, α is the high frequency gain which controls the response peak overshoot, w_c is the function crossover frequency, ζ_1 and ζ_2 are the damping ratios of crossover frequency, w_{bc} is the controller bandwidth, M_u is the magnitude of KS, and ε is a small value.

B. CONTROLLER DESIGN

The H_∞ controller was designed so that H_∞-norm from input $w=F_d$ to output $z=\begin{bmatrix}e_p\\ e_u\end{bmatrix}$ is minimized.

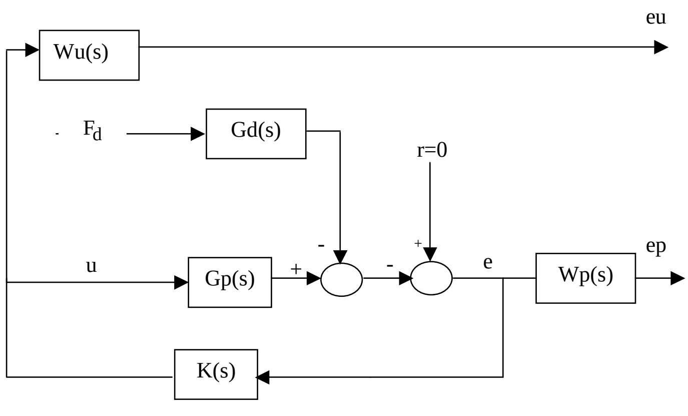

Fig. 8. The standard feedback diagram of the system with weights

Where F_d is the input disturbance signal, e_p, e_u are the weighted error and control signals. Fig. 8 shows the standard feedback diagram of the system with weights. The generalized plant *P* is expressed by:

$$\begin{bmatrix} e_p \\ e_u \\ e \end{bmatrix} = \begin{bmatrix} W_p G_d & -W_p G_p \\ 0 & W_u \\ G_d & -G_p \end{bmatrix} \begin{bmatrix} F_d \\ u \end{bmatrix} \quad (33)$$

where *u* is the control signal.

The lower linear fractional transformation of the generalized plant *P* and controller $K(s)$ can be described by:

$$F_l(P,K) = \begin{bmatrix} W_p G_d S \\ W_u G_d KS \end{bmatrix} \quad (34)$$

The objective of H_∞ control is to find the controller *K(s)* that internally stabilizes the system such that $\|T_{zw}(s)\|_\infty$ is minimized [3]. Where $\|T_{zw}\|_\infty$ is the transfer function of the system from input *w* to output *z* and can be expressed as:

$$\|T_{zw}\|_\infty = \left\| \begin{bmatrix} W_p G_d S \\ W_u G_d KS \end{bmatrix} \right\|_\infty \quad (35)$$

The H_∞ control minimizes the cost function in equation (35) using γ-iteration [17] to find the stabilizing controller such that $\|T_{zw}\|_\infty < \gamma$. To find the optimal value of γ, the PSO algorithm was used to tune the parameters of the selected weighting functions. The weighting functions have a significant effect on the overall design of H_∞ control technique.

The optimal value of γ is the infimum overall γ such that the H_∞ control conditions are satisfied. A suboptimal H_∞ controller was obtained using the following Matlab command:

$$>>[K, T_{zw}, \gamma_{suboptimal}] = h\inf syn(P, n_y, n_u, \gamma_{\min}, \gamma_{\max}, tol) \quad (36)$$

where n_y and n_u are the dimensions of y_p and *u*, $\gamma_{\min}$ and $\gamma_{\max}$ are the lower and upper bound for $\gamma_{optimal}$, and *tol* is the tolerance to the optimal value.

The fitness function used in PSO algorithm is the performance criteria stated in equation (35). The algorithm obtains the minimum value of the infinity norm of the performance criteria from the search space that minimizes the objective function in equation (35). The following parameters have been used for carrying out the QFT controller design using PSO:

i) The members of each individual in the PSO algorithm are β, α, w_c, ζ_1, ζ_2, w_{bc}, M_u.
ii) Population size equal to 100.
iii) Inertia weight factor $h = 2$.
iv) $c_1 = 2$ and $c_2 = 2$.
v) Maximum iteration is set to 100.

The PSO steps for obtaining the optimal parameters of the proposed controller can be summarized as:

1. Define the system model, $G_p(s)$.
2. Define the structure of W_p, W_u according to equations (31) and (32).
3. Initialize the individuals of the population randomly in the search space.
4. For each initial of the population (vector of the parameters to be optimised), determine the fitness function in equation (35).
5. Compare each value of equation (35) with its personal best x_i. The best value among the x_i is denoted as x_i^g.
6. Update the velocity of each individual according to (2).
7. Update the position of each individual according to (1).
8. If the number of iterations reaches the maximum, then go to step 9, otherwise, go to step 4.
9. The latest x_i^g is the optimal parameters of the weighting functions.

The proposed PSO algorithm for obtaining the optimal values of the weighting functions parameters is described by the flowchart shown in Fig. 9. The overall block diagram of the system with PSO tuning algorithm is shown in Fig. 10.

The interval for γ iteration was selected between 0.1 and 10. The obtained controllers for the two cases of load variation range, respectively, are:

$$K(s) = \frac{2.797s^2 + 598.6s + 3.203\times10^5}{s^3 + 7035s^2 + 2.422\times10^5 s + 3.222\times10^6} \quad (37)$$

$$K(s) = \frac{2.021s^4 + 90.13s^3 + 6568s^2 + 6.191\times10^4 s}{s^5 + 2383s^4 + 5.195\times10^4 s^3 + 4.236\times10^5 s^2 + 1.444\times10^6 s + 5.588\times10^4} \quad (38)$$

The optimal weighting functions parameters obtained with $\gamma = 0.8559$ using PSO algorithm are shown in Table II.

V. RESULTS AND DISCUSSION

Fig. 11 shows the singular values of the closed loop system with the controller $K(s)$. As is seen, the maximum value of the closed loop system is less than one, that is, the condition "$\|W_p(1+G_pK)^{-1}\|_\infty < 1$" has been satisfied. This can be checked by computing the sensitivity function of the closed loop system and comparing it with the inverse of the performance weighting function as shown in Fig. 12. It is clear that the sensitivity function lies below the inverse of W_p, which means that the performance criterion was satisfied. Fig. 13 shows the frequency response of the open loop uncertain system with the controller. From this plot, it can be seen that the minimum gain and phase margins that have been satisfied for the system with small and wide ranges of load variation are 14.1 dB, 60.6° and 12.6 dB, 55.9°, respectively. This means that the system is stable with all parameters uncertainty, that is, the robust stability has been satisfied. The time response characteristics of the closed loop nominal and uncertain systems are shown in Figs. 14 and 15, respectively. From these figures it can be seen that the time response specifications that have been achieved for the two cases of load variation range are: rise time=0.239 s, settling time (2%)=0.498 s, maximum overshoot=10% for the case of small range of load variation and rise time=0.573 s, settling time (2%)=1.18 s, maximum overshoot =11% for the case of wide range of load variation.

The time response characteristic of the system subjected to disturbance is shown in Fig. 16.

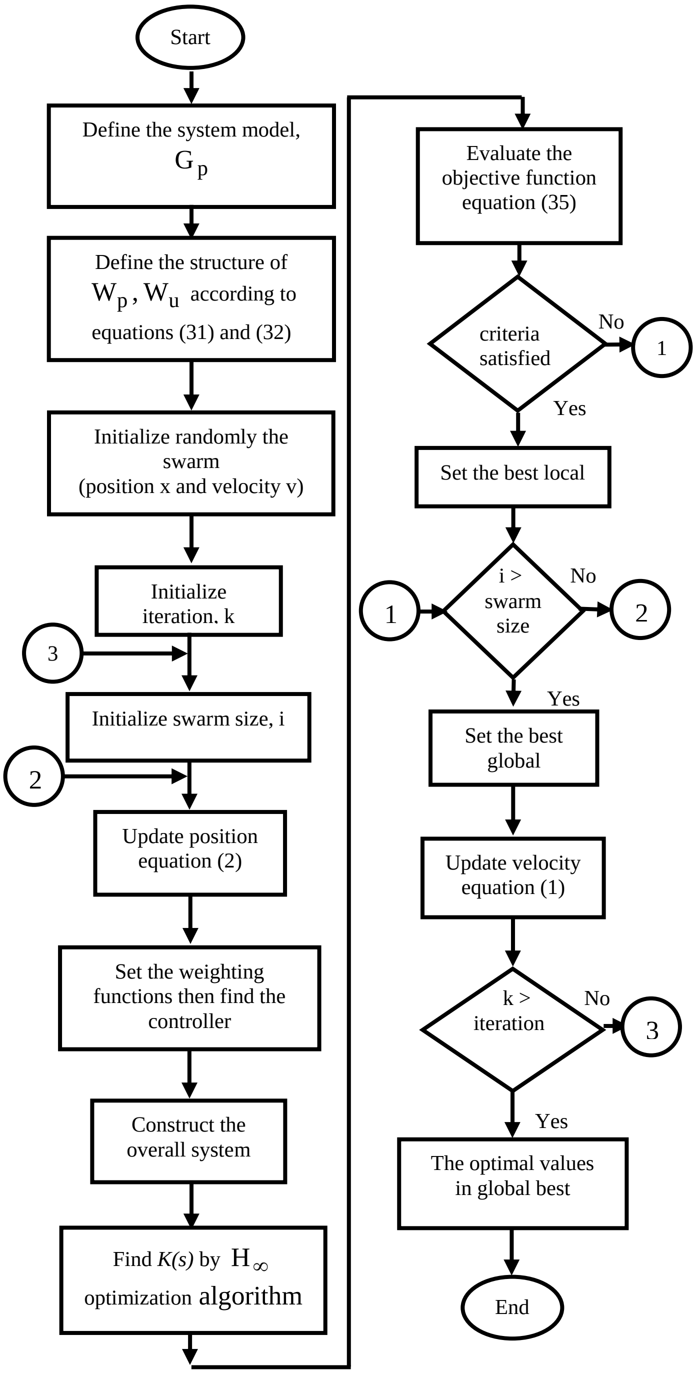

Fig. 9. Flowchart for tuning the weighting functions using PSO

It shows that the disturbance attenuation specifications have been met. For practical requirements, it is required that the control signal be small to avoid the problem of saturation. Fig. 17 shows the frequency characteristics of the control signal where a small magnitude maximum value has been obtained. However, for discretizing the system and the obtained controllers, the Zero-Order-Hold and Bilinear Transformation methods were used, respectively. With a sampling time, $T_s = 0.02$ s, the following discrete controllers for small and wide ranges of load variation were obtained, respectively:

$$K(z) = \frac{0.004131(z+1)(z^2+1.433z+0.706)}{(z+0.9187)(z^2-1.371z+0.5036)} \quad (39)$$

$$K(z) = \frac{0.0011952(z+1)(z-1)(z-0.8083)(z^2-0.873z+0.5826)}{(z+0.9187)(z-0.8141)(z-0.9992)(z^2-1.771z+0.7925)} \quad (40)$$

Fig. 18 shows the discrete time response specifications of the controlled system.

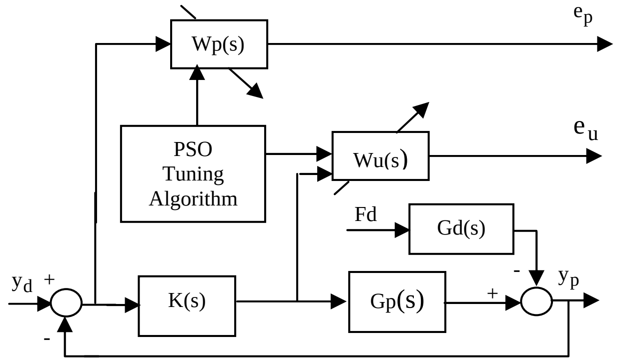

Fig. 10. Block diagram of the overall controlled system

Table II. Optimal parameters of weighting functions

Parameter	Small range of load variation	Wide range of load variation
β	90.5	60.5
α	0.01	0.01
w_c	5	4.93
ζ_1	1.38	0.38
ζ_2	8.12	8.1242
w_{bc}	10.7	1.7
M_u	1	1.00112

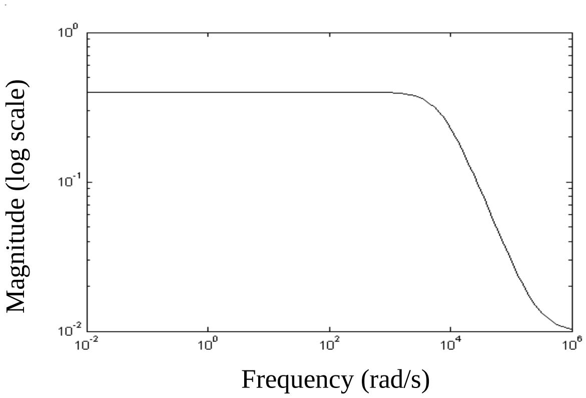

(*a*)

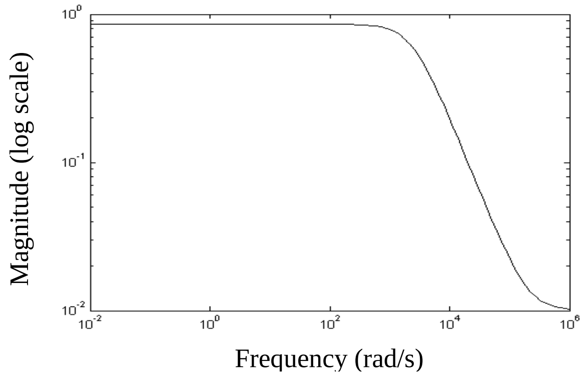

(*b*)

Fig. 11. The largest singular Value of the closed loop controlled system
a) in case of small range of load variation b) in case of wide range of load variation

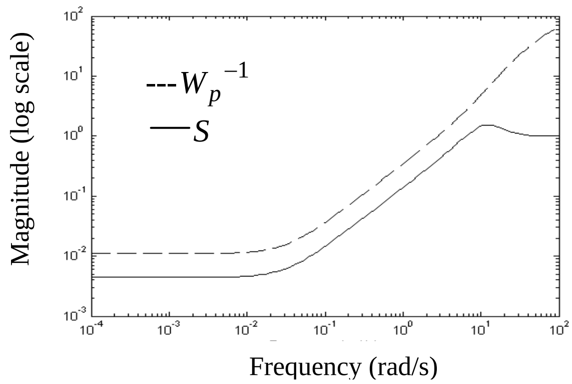

(*a*)

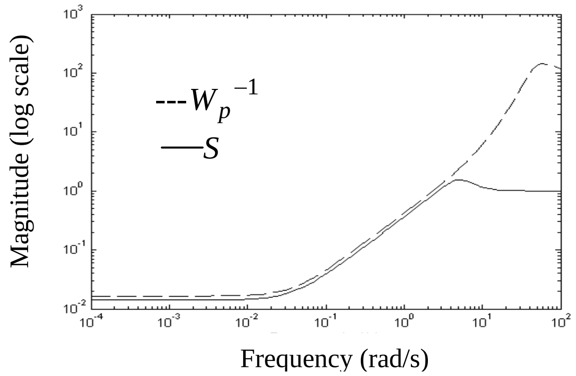

(*b*)

Fig. 12. Frequency characteristics of sensitivity function *S* and the inverse of the weighting function a) in case of small range of load variation b) in case of wide range of load variation

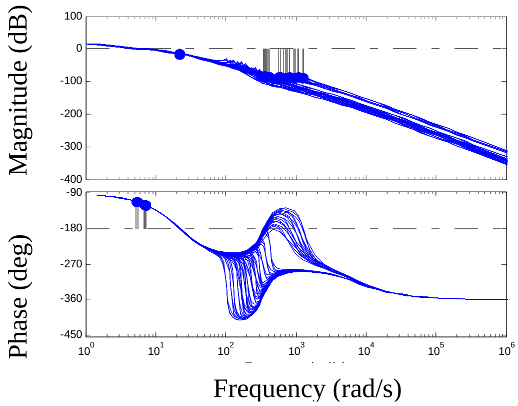

(*a*)

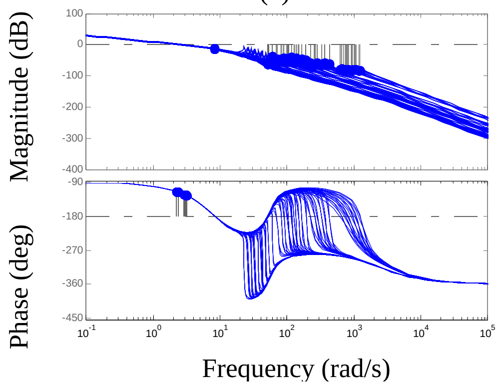

(*b*)

Fig. 13. Frequency response characteristics of the uncertain controlled system a) in case of small range of load variation b) in case of wide range of load variation

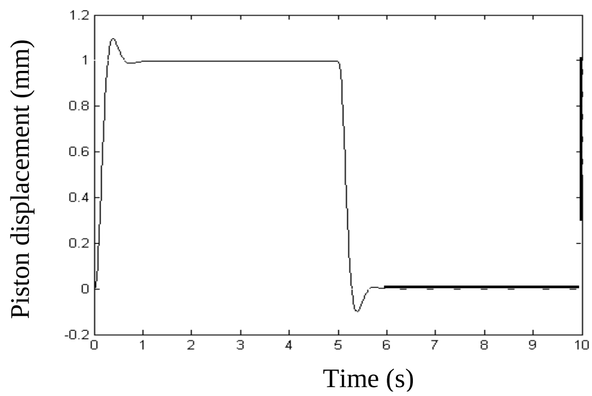

(*a*)

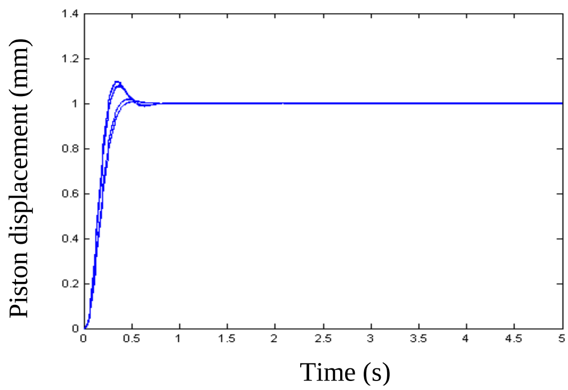

(*b*)

Fig. 14. Closed loop time response characteristics of the controlled system in case of small range of load variation a) nominal plant b) uncertain plant

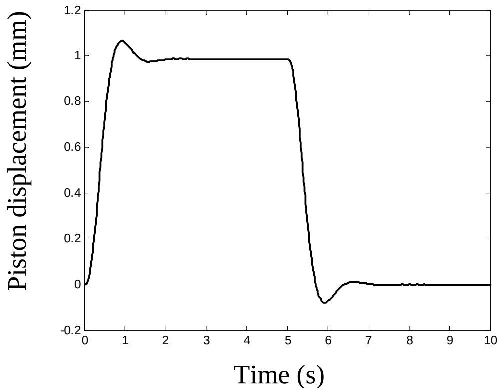

(*a*)

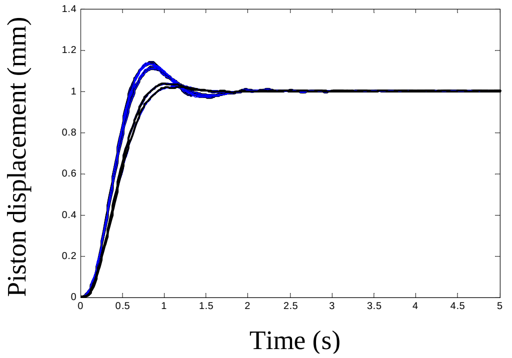

(*b*)

Fig. 15. Closed loop time response characteristics of the controlled system in case of wide range of load variation with structured uncertainty a) nominal plant b) uncertain plant

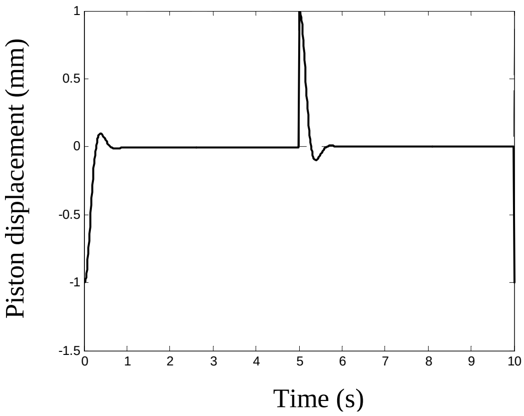

(*a*)

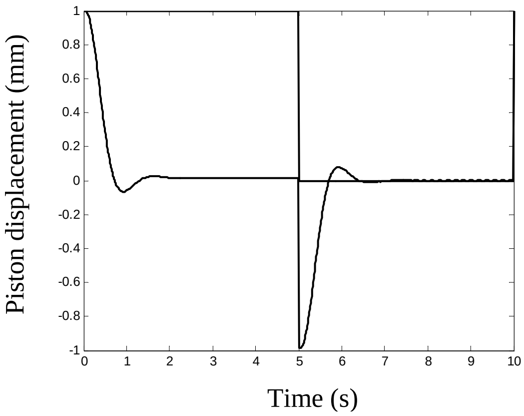

(*b*)

Fig. 16. Time response characteristics of the closed Loop controlled system subjected to disturbance
a) in case of small range of load variation b) in case of wide range of load variation

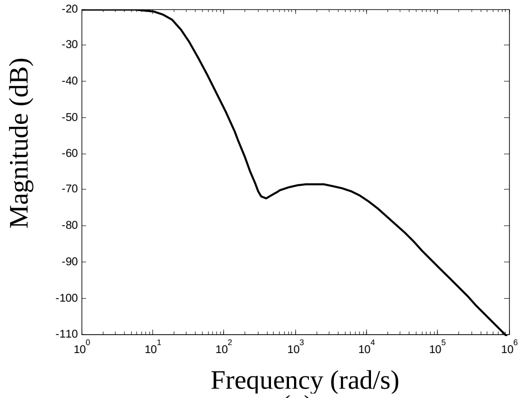

(*a*)

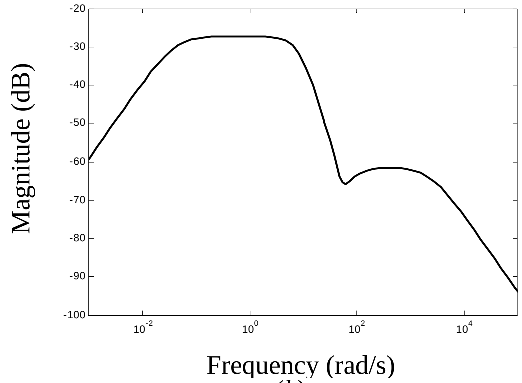

(*b*)

Fig. 17. Frequency response characteristics of the control signal
a) in case of small range of load variation b) in case of wide range of load variation

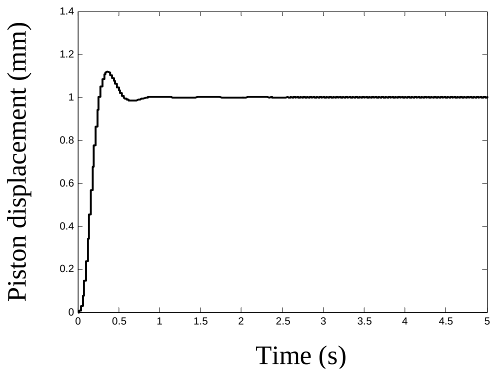

(*a*)

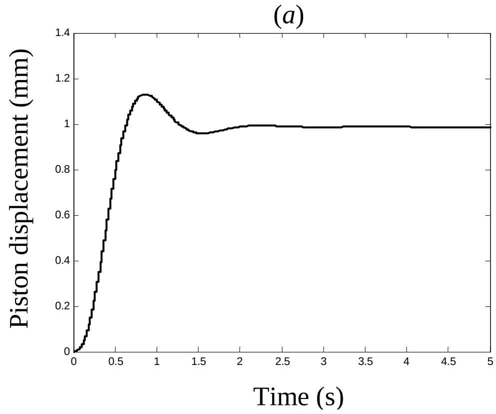

(*b*)

Fig. 18. Discrete closed loop time response characteristics of the controlled system a) in case of small range of load variation b) in case of wide range of load variation

VI. CONCLUSION

In this paper, an H_∞ controller was designed to assure robust stability and robust performance of the uncertain pneumatic servo actuator system with small and wide ranges of load variation. The H_∞ controller was designed using structured (parametric) uncertainty to achieve robust stability and performance of the system. The two cases of load variation range have been considered in the design.

Suitable formulas for performance and control weighting functions have been selected for controller design requirements. The particle swarm optimization algorithm (PSO) was used to tune the performance and control weighting functions by minimizing the infinity norm of the transfer function matrix of the nominal closed loop system. The use of the PSO method simplified the design procedure to obtain the optimal robust controller, which achieves the position control of the pneumatic servo actuator system.

Further, it can be concluded that the H_∞ optimal control is a powerful technique to design a robust control for the pneumatic servo actuator system with structured uncertainty and disturbances.

REFERENCES

[1] D. W. Gu, P. Hr. Petkov, and M. M. Konstantinov, "Robust control design with Matlab", Springer, 2005.

[2] S. Alok, "Linear systems optimal and robust control", Taylor and Francis Group, USA, 2007.

[3] K. Zhou, and J. C. Doyle, "Essentials of robust control", Prentice Hall, 1998.

[4] M. E. El-Telbany, "Employing particle swarm optimizer and genetic algorithms for optimal tuning of PID controllers: A comparitive study", ICGST-ACSE Journal, Vol. 7, No. 2, 2007, pp. 49-54.

[5] A. A. El-Saleh, M. Ismail, R. Viknesh, C. C. Mark, M. L. Chen, "Particle swarm optimization for mobile network design", IEICE Electronics Express, Vol. 6, No. 17, 2009, pp. 1219-1225.

[6] A. Soundarrajan, S. Sumathi and C. Sunder, "Particle swarm optimization based LFC and AVR of autonomous power generating system", IAENG International Journal of Computer Science, Vol. 37, Issue 1, pp85-92, 2010.

[7] C. –H. Yang, C. -J Hsiao and L. -Y Chuang, "Linearly decreasing weight particle swarm optimization with accelerated strategy for data clustering", IAENG International Journal of Computer Science, Vol. 37, Issue 3, pp234-241, 2010.

[8] M. Zamani, N. Sadati, M. K. Ghartmani, "Design of an H_∞ PID controller using particle swarm optimization", International Journal of Control, Automation, and Systems, Vol. 7, No. 2, 2009, pp. 273-280.

[9] B. Allaoua, B. Gasbaoui, B. Mebarki, "Setting up PID d.c motor speed control alteration parameters using particle swarm optimization strategy", Leonardo Electronic Journal of Practices and Technologies", Vol. 14, 2009, pp. 19-32.

[10] M. Karpenko, N. Sepehri, "Development and experimental evaluation of a fixed-gain nonlinear control for a low-cost pneumatic actuator", IEE Proc.-Control Theory Appl., Vol. 153, No. 6, 2006, pp. 629-640.

[11] H. I. Ali, S. B. Mohd Noor, S. M. Bashi, M. H. Marhaban, "Robust QFT controller design for positioning a pneumatic servo actuator", Proc. of student conference on research and development, Johor, Malaysia, 2008, pp. 128-1—128-4.

[12] K. Khayati, P. Bigras, L. A. Dessaint, "Force control loop affected by bounded uncertainties and unbounded inputs for pneumatic actuator systems", Journal of Dynamic systems, Measurement, and Control, Vol. 130, No. 011007, 2008, pp. 1-9.

[13] S. Qiang, L. Fang, "Two effective control algorithms for a pneumatic system", International Technology and Innovation Conference, Hangzhou, China, 2007, pp. 1980-1985.

[14] Y. Zhu, "Control of pneumatic systems for free space and interaction tasks with system and environmental uncertainties", Ph.D Dissertation, Vanderbilt University, Nashville, Tennessee, 2006.

[15] M. Karpenko, N. Sephri, "QFT design of a PI controller with dynamic pressure feedback for positioning a pneumatic actuator", Proc. of of American Control Conference, Boston, Nassachusetts, 2004, pp. 5084-5089.

[16] R. Y. Chiang and M. G. Safonov, "Matlab robust control toolbox", Mathworks, Inc., USA, 1997.

[17] Skogestad and Postlethwaite, "Multivariable feedback control-analysis and design", Wiley, 2005.

Hazem I. Ali was born in Baghdad, Iraq. He received the B.Sc and M.Sc degrees in Control and Systems Engineering from University of Technology, Baghdad, Iraq, in 1997 and 2000 respectively. From October 2002 to November 2007, he was a lecturer in the Department of Control and Systems Engineering, University of Technology, Baghdad, Iraq. Since 2008 he is a Ph.D student in the Department of Electrical and Electronic Engineering, Control and Automation Field, University Putra Malaysia, Malaysia. His current research interests include Robust control, Intelligent control, Process control.

Samsul Bahari bin Mohd Noor, graduated from University of Warwick in Electronic Engineering in 1991, and obtained his MSc and PhD in Control Engineering at Sheffield University, UK, in 1992 and 1996 respectively. He is a Senior Lecturer at the Department of Electrical and Electronic Engineering, Faculty of Engineering, UPM. He was the Head of IT unit and the Head of the Electrical and Electronic Engineering Department. Currently, he is a Deputy Dean (Development and Finance) of the Engineering Faculty and also Head of Control System and Signal Processing research area. He has been invited by the Ministry of Human Resources to develop the National Occupational Skill Standard for Process Control. He has led a few researches on Satellite Control, and Optimal and Intelligent Control of Chemical Processes, apart from being a member of research groups related to instrumentation and control. Senior Member of IEEE, Member of Technical Committee (SIRIM)(2006-date). Areas of Expertise: Control engineering, process modelling and control and instrumentation, Model Predictive Control and Intelligent Control.

Mohammad Hamiruce Marhaban, received B.Eng. in Electrical and Electronic Engineering, Universiti of Salford, UK, from 1996 to 1998. He received Ph.D degree in Electronic Engineering, Universiti of Surrey, UK, from 1999 to 2003. He is a Lecturer in Department of Electrical and Electronic Engineering, Faculty of Engineering, UPM. (May 2003 to Present), and also he is a Member of IEEE. Area of Interest: Intelligent Control System and Computer Vision.

S. M. Bashi, graduated from University of Mosul, in Electrical and Electronics Engineering (1969). He received his PhD in Simulation of power transmission system from Loughborough University of Technology, England (1980). Since 1999, he is with the Department of Electrical and Electronics Engineering, Faculty of Engineering, Universiti Putra Malaysia, Malaysia. His area of research interest includes; power system analysis and design, quality of power supply, simulation and application of power electronics systems, and machines drives.